

AD-A089 446

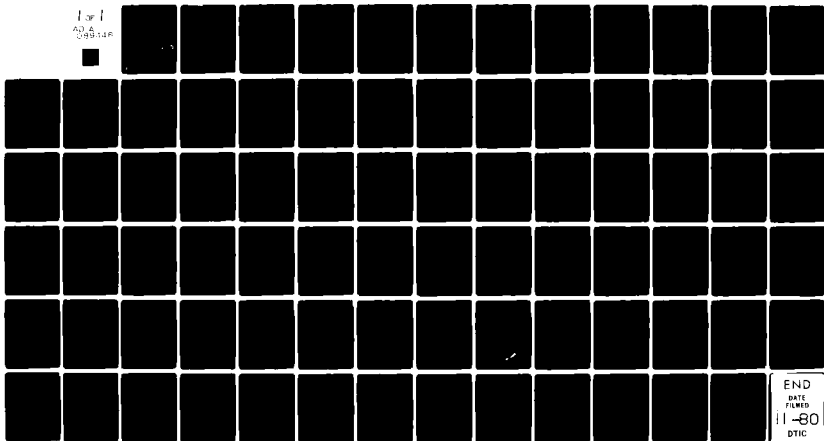
MICHIGAN STATE UNIV EAST LANSING DEPT OF BIOMECHANICS F/6 6/2
THE ACCURACY OF SCREW AXIS ANALYSIS USING POSITION DATA FROM AN--ETC(U)
MAY 80 J H MARCUS F49620-78-C-0012

UNCLASSIFIED

AFOSR-TR-80-0868

NL

1 of 1
AD-A089 446



END
DATE
FILMED
11-80
DTIC

UNCLASSIFIED

SECURITY CLASSIFICATION OF THIS PAGE (When Data Entered)

12

READ INSTRUCTIONS BEFORE COMPLETING FORM

19 REPORT DOCUMENTATION PAGE

1. REPORT NUMBER AFOSR/TR-80-0868	2. GOVT ACCESSION NO. AD-A089446	3. RECIPIENT'S CATALOG NUMBER 2
4. TITLE (and Subtitle) The Accuracy of Screw Axis Analysis Using Position Data From Anatomical Motion Studies		5. TYPE OF REPORT & PERIOD COVERED Annual Report 1 Nov. 78 - 31 Oct. 79
7. AUTHOR(s) 10 Jeffrey H. Marcus		6. PERFORMING ORG. REPORT NUMBER
9. PERFORMING ORGANIZATION NAME AND ADDRESS Department of Biomechanics Michigan State University East Lansing, Michigan 48824		8. CONTRACT OR GRANT NUMBER(s) F49620-78-C-0012 <i>new</i>
11. CONTROLLING OFFICE NAME AND ADDRESS Air Force Office of Scientific Research (NL) Bolling AFB, DC 20332		10. PROGRAM ELEMENT, PROJECT, TASK AREA & WORK UNIT NUMBERS 61102F 2313/A4 17
14. MONITORING AGENCY NAME & ADDRESS (if different from Controlling Office)		12. REPORT DATE 5 May 1980
		13. NUMBER OF PAGES 125
		15. SECURITY CLASS. (of this report) Unclassified
		15a. DECLASSIFICATION/DOWNGRADING SCHEDULE

LEVEL

New

16. DISTRIBUTION STATEMENT (of this Report)

Approved for public release;
distribution unlimited.

17. DISTRIBUTION STATEMENT (of the abstract entered in Block 20, if different from Report)

18. SUPPLEMENTARY NOTES

19. KEY WORDS (Continue on reverse side if necessary and identify by block number)

Screw Axis; Kinematics; Human Joint Mobility; Error Analysis

411935

20. ABSTRACT (Continue on reverse side if necessary and identify by block number)
Research involving the kinematics of human joint mobility often involves screw axis analysis. As a prelude to such research a screw axis analysis program was developed and implemented for use in the Systems Anthropometry Laboratory. This report presents a detailed discussion of the algorithm used to find Displacement Matrices (DM) and screw axis parameters. Error propagation due to uncertainty in DM is analytically developed and then demonstrated. The rotation angle is found to be the most critical screw axis parameter, and the components of a unit vector in the direction of the screw axis are the most sensi-

(see attachment)

DTIC ELECTED
SEP 24 1980

AD A 089446

UUC FILE COPY

tive to error. Using the condition number of a matrix, a method is developed and presented for evaluating the error propagation due to the matrix operations used to find DM.



Accession For	
NTIS GRA&I	<input checked="" type="checkbox"/>
DDC TAB	<input type="checkbox"/>
Unannounced	<input type="checkbox"/>
Justification	
By _____	
Distribution/	
Availability Codes	
Dist	Avail and/or special
PI	

Unclassified

ACKNOWLEDGEMENTS

One of the more educational parts of writing this thesis has been learning how indebted I am for the help people have given me. I would like to thank my advisor, Dr. James Bernard, for all his help. Dr. H. M. Reynolds, who I have worked so closely with these last two years, is the person who introduced me to the challenges of working with biological systems. Dr. Robert Hubbard listened to various ideas I had for my thesis, from the flailing for a subject stage through his helpful reviews of this thesis. These three men, who served on my committee, are the people who introduced me to serious technical writing, which I discovered to be quite different from my previous background in rhetorical and political writing.

When I wondered about matrix theory I consulted with Mr. Joseph Whitesell. His quick grasp of the mathematics of a problem helped me on many occasions in the preparation of this thesis.

None of the work done for this thesis would have been possible had not the United States Air Force funded this project under contract AFOSR-F49620-78-C-0012. The support given me by the Department of Biomechanics of the College of

AIR FORCE OFFICE OF SCIENTIFIC RESEARCH (AFSC)
NOTICE OF TRANSMITTAL TO DDC
This technical report has been reviewed and is approved for public release IAW AFR 190-18 (7b). iii
Distribution is unlimited.
A. D. BLOSE
Technical Information Officer

Approved for public release;
distribution unlimited.

Osteopathic Medicine of Michigan State University is also gratefully acknowledged.

Jim Freeman and Kathy Hornback worked with me on the many mysteries of computer science, and helped me with some of my programming needs.

To all of these people, thank you.

TABLE OF CONTENTS

	Page
LIST OF TABLES	viii
LIST OF FIGURES	xi
LIST OF SYMBOLS	x
INTRODUCTION	1
BACKGROUND AND LITERATURE REVIEW	3
2.1 Literature Review	3
2.2 The Systems Anthropometry Laboratory.	6
DESCRIPTION OF THREE DIMENSIONAL MOTION	11
3.1 Introduction.	11
3.2 Displacement Matrices	12
3.3 Computation of DM from Position Data.	14
3.4 Determining the Screw Axis Parameters from DM	15
3.5 Relationship to the Eigenvalue Problem.	21
THREE DIMENSIONAL POSITION DESCRIPTION.	22
4.1 Introduction.	22
4.2 Algorithm for Setting Up a Coordinate System Based on Three Data Points	24
4.3 Effect of Errors on Coordinate System Determination	26

TABLE OF CONTENTS (Con't)

	Page
ERROR ANALYSIS.	28
5.1 How Errors in Position Effect DM.	28
5.2 How Errors in DM Effect the Screw Axis.	33
5.3 Conclusion.	40
EVALUATION OF THE ACTUAL EFFECT OF ADDING ERRORS. . .	41
6.1 Introduction and Description of Procedure	41
6.2 Results	42
6.3 Discussion.	49
6.4 Evaluating Cond (Pl).	51
EXAMPLE OF SCREW AXIS ANALYSIS USING ANATOMICAL DATA.	54
7.1 Introduction.	54
7.2 Discussion.	56
SUMMARY, REVIEW, AND RECOMMENDATIONS.	59
8.1 Summary and Review.	59
8.2 Is the Condition Number of a Matrix of Any Use?.	61
8.3 Recommendation for Future Work.	63
8.4 Conclusions	67
LIST OF REFERENCES.	69

55- blank

LIST OF TABLES

Table		Page
5-1	Effect of Significant Figures on Small Angles.	32
6-1	Error With $\phi=1^\circ$; 4 Significant Figures	40
6-2	Error With $\phi=1^\circ$; 5 Significant Figures	41
6-3	Error With $\phi=5^\circ$; 4 Significant Figures	42
6-4	Error With $\phi=10^\circ$; 4 Significant Figures.	43
6-5	Error With $\phi=60^\circ$; 4 Significant Figures.	44
6-6	Summary of Error Analysis.	45
7-1	Screw Axis Analysis for Hip Motion	57
7-2	Screw Axis Analysis for the Sacro-iliac Joint. .	57

LIST OF FIGURES

Figure	Title	Page
2-1	Systems Anthropometry Data Collection and Analysis System.	7
2-2	Basic Stereo-Radiographic Configuration for Systems Anthropometry Laboratory	8
4-1	Data Based Coordinate System.	25
5-1	Rotation Angle Versus Error in Rotation Angle.	35

LIST OF SYMBOLS

- a_{ij} - the i j th entry in DM
- A - a matrix which is known in a system of linear equations
- \bar{A} - a three dimensional point on a rigid body
- $\bar{A1}$ - point A at rigid body position 1
- $\bar{A2}$ - point A at rigid body position 2
- \overline{AB} - a vector from point A to point B
- $\overline{AB1}$ - vector AB at rigid body position 1
- $\overline{AB2}$ - vector AB at rigid body position 2
- \overline{AC} - vector from point A to point C
- b - the matrix on the right hand side of the standard equation $Ax=b$ of a system of linear equations
- \bar{B} - a three dimensional point on a rigid body
- \bar{C} - a three dimensional point of a rigid body
- $C\phi$ - cosine of angle ϕ
- $\text{cond}(A)$ - condition number of a matrix A; the euclidean norm of A times the euclidean norm of A^{-1}
- \bar{D} - a three dimensional point on a rigid body
- DM - Displacement Matrix
- DOF - degrees of freedom
- e_i - error in some parameter i ; may be a matrix or a scalar depending on context
- i - unit vector in x direction
- j - unit vector in y direction
- k - unit vector in z direction

- I - the identity matrix; a matrix which is 0 everywhere except the diagonal which is all 1's
- ISA - instantaneous screw axis
- \overline{Or} - origin of new coordinate system
- P1 - a 4x4 matrix describing the position of a rigid body at time 1
- P2 - a 4x4 matrix describing the position of a rigid body at time 2
- RM - Rotation Matrix
- s - translation parallel to the screw axis
- S ϕ - sine of angle ϕ
- Tr_{RM} - trace of RM; sum of the diagonal entries of RM
- \bar{U} - unit vector in the direction of the screw axis
- u_x - x component of U
- u_y - y component of U
- u_z - z component of U
- V ϕ - vers of ϕ ; 1-cos ϕ
- θ - an angle, particularly between relative position vectors
- ϕ - rotation angle in screw axis analysis
- $\sum_{i=j}^{i=n}$ - summation from i=j to i=n
- |AB| - magnitude of some vector AB; the square root of the sum of the squared components of a vector
- ||A|| - Euclidean norm of a matrix A; the square root of the sum of squared components of a matrix

CHAPTER 1

INTRODUCTION

Recently the need and capability to describe human joint mobility has prompted studies into the kinematics of joint motion. Particularly since the 1960's when the advent of large digital computers made complicated three dimensional kinematic analysis practical, there has been an expansion of research aimed at creating the elements of a model for describing human body motion.

The kinematics of body motion often involves complicated three-dimensional displacement descriptions. One commonly used method of three-dimensional kinematic analysis is the screw axis. By describing a displacement with a single translation and a single rotation, screw axis analysis aids in understanding how parts of the body move during a particular displacement.

The Systems Anthropometry Laboratory is a new facility dedicated to the study of human body motion. Screw axis analysis is used as a part of these studies, but how accurately can a body displacement be described by the screw axis? The displacement descriptions are derived from empirical data such as position descriptions. Measurement errors, which are present in empirical data, will propagate through

the kinematic analysis. Even if there are no measurement errors, the number of significant figures affects the calculations.

This thesis will examine the limitations and requirements for accuracy in the kinematic analysis of human body motion. Two different but related questions will be examined. First, how do measurement errors in position data propagate through the computation of Displacement Matrices? The second question is, given some error in the Displacement Matrix, how is the screw axis affected? Along with measurement errors, the number of significant figures in the Displacement Matrix may limit the screw axis analysis.

In summary, the limitations on Displacement Matrices due to measurement errors, and the limitations on screw axis analysis due to the Displacement Matrix will be considered in the following pages.

CHAPTER 2

BACKGROUND AND LITERATURE REVIEW

2.1 Literature Review

Many situations encountered in design require a knowledge of the position and motion of the human body. Examples include the design of vehicles for situations where large dynamic forces are encountered, as in a crash. The design of a chair requires knowledge of the interaction between the chair and the person sitting in it. A prosthesis, such as an artificial hip, must accurately reproduce the function of the replaced part. Further applications are in workspace definition. If a driver cannot reach the controls of a car when wearing a shoulder harness, he is not likely to use the shoulder harness.

Traditionally, the human body is modelled using rigid body mechanics. By dividing the body into a series of "mass links", and connecting these links with a number of different types of joints, a kinematic model of the body is created. In the late 1800's Braune and Fisher {3,4,5} laid the foundation for this approach when they investigated the biomechanics of the body positions assumed by German infantrymen. The technique of using mechanical analogues of human anatomy, such as the "mass link", was continued into

the 20th century. Dempster [8,9] achieved the most extensive results in 1955, and much of his data is still in use. Much of Dempster's research in body mobility concerns locating a path of instantaneous joint centers of rotation, which is a two-dimensional description of body motion.

Dempster and other investigators prior to the 1960's used the two-dimensional kinematics of Reuleaux [19]. Three-dimensional kinematics existed, indeed Chasles [7] described the screw axis theorem in 1830, but analytical methods were cumbersome and impractical until the advent of large digital computers in the 1960's. Potthoff [18] was among the first to apply the more sophisticated kinematic analysis made possible by computers. Potthoff tried to analyze Braune and Fisher's data using the screw axis theorem, but found that their data was not accurate enough for screw axis analysis.

Braune and Fisher's data were taken from surface targets on the skin of a person. Emanuel and Barter [10] found that targets placed on human skin do not maintain a stable position relative to the skeleton, or relative to other targets on the skin, and thus violate the rigid body assumption of the "mass link" concept. Measurement techniques not relying on surface targets were developed and used in the late 1960's and early 1970's. Thompson [28] and Kinzel [13,15] used instrumented linkages to describe the relative motion between body segments. Both Thompson and

Kinzel used screw axis analysis, with Thompson reporting that an averaging technique was necessary before accurate results could be obtained. Kinzel optimized his linkage and reported use of the screw axis with confidence, but he too noted its sensitivity to error.

The use of the "mass link" concept requires knowledge of the characteristics of the joints which connect the "mass links." The least constrained joint model is the spatial joint, which allows translation in all three coordinate directions, and rotation around each of the three coordinate axes. A spatial joint is, therefore, a full three-dimensional six degree of freedom* joint, and the resulting kinematic analysis is complicated. Researchers often make assumptions to reduce the degrees of freedom and thus simplify the analysis. Kinzel [13] has identified five joint models commonly reported or implied in the literature. These five are:

- 1) the one DOF hinge, or revolute joint
- 2) the three DOF planar joint
- 3) the three DOF spherical, or ball and socket joint
- 4) the two DOF spherical joint
- 5) the six DOF spatial joint

Kinzel discusses each of these in detail. Kinzel also states "all anatomical joints permit six degrees of freedom to some extent." The implication is that use of a joint model

*degree of freedom, or DOF, is defined as the minimum number of independent parameters required to completely define the relative position or displacement of one member relative to another [13].

other than a spatial model is unduly restrictive.

While Thompson and Kinzel used instrumented linkages to describe anatomical motion, others {6,12,17,21,26} were investigating the use of stereo-radiography. The most nearly rigid part of the anatomy is bone, and most single bones are essentially rigid bodies under the forces normally encountered in the body. Because radiography allows the determination of a bone's position in vivo, and bones are essentially rigid bodies, rigid body position data may be obtained. The utility of stereo-radiography is its ability to accurately determine the three-dimensional coordinates of a target on a bone. Other methods such as instrumented linkages must contend with the problems due to skin not being a rigid body.

2.2 The Systems Anthropometry Laboratory

The Systems Anthropometry Laboratory (SAL) {20,21,22,23} of the Department of Biomechanics, College of Osteopathic Medicine at Michigan State University is a new facility for obtaining accurate and repeatable data relating to the kinematics of human joint mobility. Through the use of stereo-radiography {21,22,23} the relative movement between bones, or the absolute position of a bone with respect to an inertial axis system may be measured. Body position and mobility are studied from the viewpoint that the human body is a three dimensional system composed of links connected by joints with six DOF {23}.

As a bone is moved, the use of stereo-radiography allows

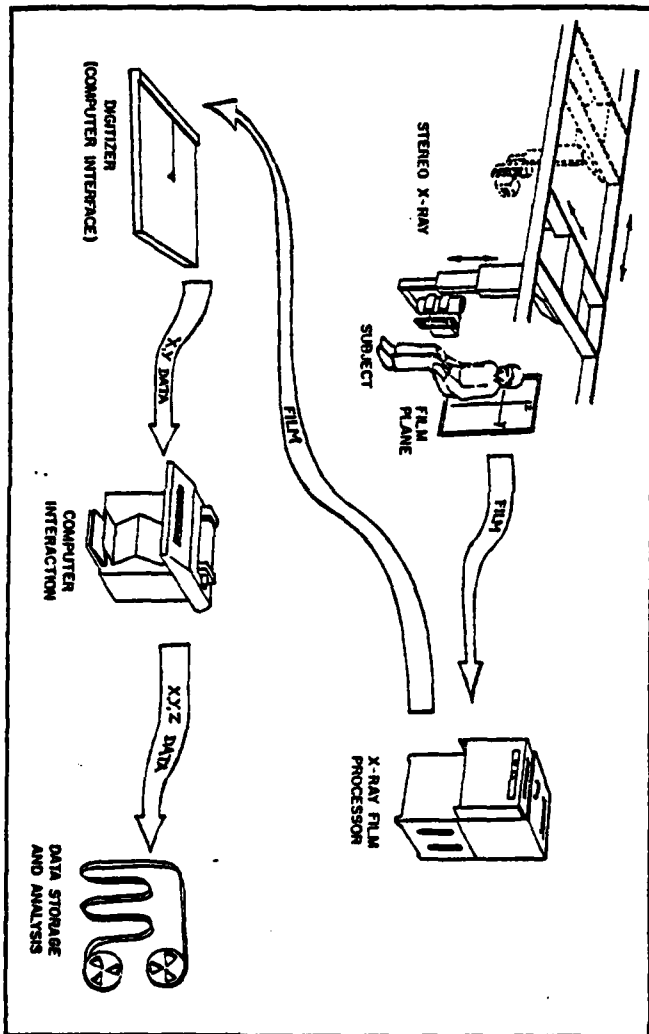


FIGURE 2-1 Systems Anthropometry Data Collection and Analysis System

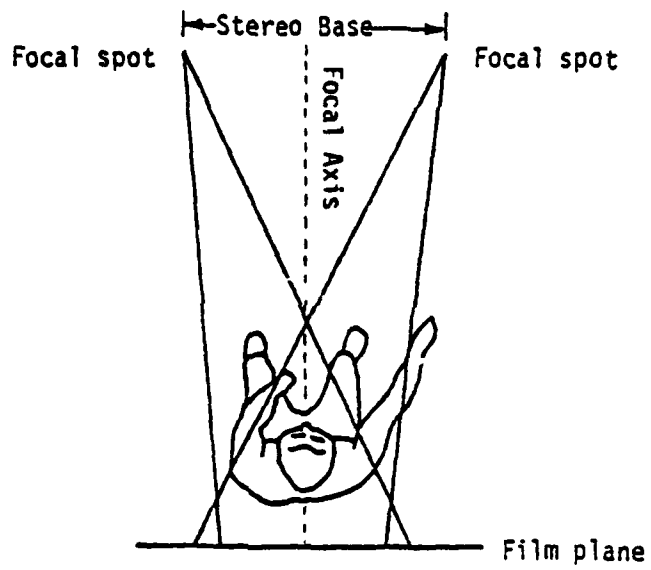


FIGURE 2-2 Basic Stereo-Radiographic Configuration for Systems Anthropometry Laboratory

the measurement of the position of the bone. Since large doses of X-ray radiation are required, cadavers are used for the joint mobility studies. Thus there is no restriction, based on radiation exposure limits, on the number of radiographs which can be obtained. Embalming tends to make cadavers unnaturally stiff, so only fresh, unembalmed cadavers are used.

A joint mobility study begins by imbedding X ray targets, tungsten-carbide balls .8mm in diameter, in a bone near a skeletal landmark. Figure 2-1 shows the subsequent steps involved in collecting the data. The cadaver is placed between the X-ray tubes and the film holder, as illustrated in Figure 2-2.

Two X-ray tubes are mounted a fixed distance apart. At each step in the movement of the cadaver's joint, a film is loaded into the film holder. One of the X-ray tubes then "fires," exposing the film. The film is changed and the other X-ray tube "fires," exposing the second film from a different angle. The two pieces of exposed film are called a stereo pair, and contain all the information necessary to determine the three-dimensional coordinates of the X-ray targets in the cadaver. Large film sizes of 14" x 36" are used to allow the imaging of an entire "mass link" with all anatomical targets, such as the femur, on one piece of film.

Between the cadaver and the film holder is a grid of tungsten wires which define an inertial axis system. Devices on the film holder create images which can be used

to determine the geometry of the film holder relative to the X-ray tubes. The film holder is free to move between the two exposures of a stereo pair. To aid in imaging the bone, the film holder may translate in a plane parallel to the wire grid, and the film holder may rotate in the same plane around an axis normal to the wire grid.

Once the film is developed it is placed on an X-Y digitizer, which is accurate to within ± 0.013 cm. The output from the digitizer, the coordinates of a digitized image, are then processed through an algorithm which computes the three-dimensional coordinates of the target. The coordinates are reported in the inertial axis system defined by the wire grid.

To summarize, radiopaque targets implanted on a bone are tracked as the bone is moved through a series of finite steps representative of the joint's mobility. Radiographs of the targets on the bone are digitized for later use and study.

CHAPTER 3
DESCRIPTION OF THREE-DIMENSIONAL MOTION

3.1 Introduction

The description of three-dimensional motion involves a 4×4 matrix called the Displacement Matrix (DM). All information necessary to describe a three-dimensional displacement of a rigid body is contained in DM. Screw axis analysis is an attempt to put DM into a form more easily understood.

For a change of position of a rigid body there exists a unique instantaneous screw axis (ISA) {7}. The ISA is simply a line in space. All points on the rigid body may be thought of as translating parallel to the screw axis by an equal amount s , and rotating around the screw axis by an angle ϕ . The screw axis analysis describes displacement in terms of two vector quantities and two scalars. The two scalars are the translation s , and the rotation ϕ . The vector quantities are a unit vector \bar{U} in the direction of the screw axis, and the position vector of a point \bar{A} which fixes the screw axis in space. All of these parameters are found from DM, but not all of the parameters are independent. There are eight parameters for screw axis analysis (s, ϕ , three in \bar{U} , and three in A), but since this is six DOF

displacement, only six are independent.

3.2 Displacement Matrices

If \bar{A} is a point on a rigid body, and \bar{A} is known at two different positions 1 and 2, then there exists a linear transformation which maps \bar{A} from 1 to 2. This linear transformation, called the Displacement Matrix by Suh and Radcliffe {27}, is defined as follows:

$$DM \quad \bar{A}_1 = \bar{A}_2$$

where:

\bar{A}_1 is the position vector of a point A at rigid body position 1

\bar{A}_2 is the position vector of a point A at rigid body position 2

Point \bar{A} is expressed in homogeneous coordinates. The need for homogeneous coordinates arises from the fact that in order to fully describe an object in n dimensional space, n+1 coordinates are needed. The subject of homogeneous coordinates is treated in computer graphics, and a typical text is Rogers and Adams {25}. Insight into the need for an n+1 system for n dimensional space can be attained from the classic text FLATLAND {1}. The fourth coordinate for a three-dimensional system is arbitrary and usually 1. Thus \bar{A}_2 in homogeneous coordinates is

$$\overline{A2} = \begin{bmatrix} A2_x \\ A2_y \\ A2_z \\ 1 \end{bmatrix}$$

DM may be partitioned as follows:

$$\begin{bmatrix} \text{DM} \end{bmatrix} = \begin{bmatrix} a_{11} & a_{12} & a_{13} & | & a_{14} \\ a_{21} & a_{22} & a_{23} & | & a_{24} \\ a_{31} & a_{32} & a_{33} & | & a_{34} \\ \text{---} & \text{---} & \text{---} & | & \text{---} \\ a_{41} & a_{42} & a_{43} & | & a_{44} \end{bmatrix} \quad (3.2)$$

where for homogeneous coordinates

$$a_{41}=a_{42}=a_{43}=0.0 \text{ and } a_{44}=1.0$$

The upper 3 x 3 represents a rotation matrix (RM), while the last column has information about the translation. If there is no translation of the rigid body,

$$a_{14}=a_{24}=a_{34}=0.0$$

and

$$\text{RM } \overline{A1} = \overline{A2} \quad (3.3)$$

If no rotation occurs then $\text{RM} = I$, the identity matrix. Note that for equation (3.3) both $\overline{A1}$ and $\overline{A2}$ are not in

homogeneous coordinates, and are simply position vectors with x , y , and z components. Unless otherwise stated in this thesis, all position vectors and position matrices are in homogeneous coordinates.

3.3 Computation of DM for Position Data

If the coordinates of a rigid body are known at two different positions, DM can be computed. Assume there are four points \bar{A} , \bar{B} , \bar{C} , \bar{D} in homogeneous coordinates at two different positions 1 and 2. Then the following is true {27}:

$$\begin{bmatrix} DM \end{bmatrix} \begin{bmatrix} A1_x & B1_x & C1_x & D1_x \\ A1_y & B1_y & C1_y & D1_y \\ A1_z & B1_z & C1_z & D1_z \\ 1.0 & 1.0 & 1.0 & 1.0 \end{bmatrix} = \begin{bmatrix} A2_x & B2_x & C2_x & D2_x \\ A2_y & B2_y & C2_y & D2_y \\ A2_z & B2_z & C2_z & D2_z \\ 1.0 & 1.0 & 1.0 & 1.0 \end{bmatrix} \quad (3.4)$$

or

$$DM \quad P1 = P2 \quad (3.5)$$

Post multiply both sides by $P1^{-1}$ to get:

$$DM = P2 \quad P1^{-1} \quad (3.6)$$

where:

$P1$ is a 4×4 matrix describing the first position of the rigid body

P2 is a 4 x 4 matrix describing the second position of the rigid body

Thus DM may be found directly from three-dimensional empirical data in homogeneous coordinates. In this example it has been assumed that four points are specified. In fact, only three non-collinear points are needed. A fourth point may be created at each position by point \bar{C} 90° about an axis from \bar{A} to \bar{B} . Alternatively, a coordinate system based on the three non-collinear data points may be set up. Four new points are then available, one on each axis, and the origin. Once DM is calculated the parameters which specify the screw axis can be determined.

3.4 Determining The Screw Axis Parameters from DM

In this section an algorithm for determining the screw axis parameters is presented. This algorithm is based on a method presented by Suh and Radcliffe [27]. Begin with the Rotation Matrix, which is the upper 3 x 3 partition in equation (3.2).

$$RM = \begin{bmatrix} u_x^2 V\phi + C\phi & u_x u_y V\phi - u_z S\phi & u_x u_z V\phi + u_y S\phi \\ u_x u_y V\phi + u_z S\phi & u_y^2 V\phi + C\phi & u_y u_z V\phi - u_x S\phi \\ u_x u_z V\phi - u_y S\phi & u_y u_z V\phi + u_x S\phi & u_z^2 V\phi + C\phi \end{bmatrix} \quad (3.7)$$

$$V\phi = 1 - \cos\phi$$

$$C\phi = \cos\phi$$

$$S\phi = \sin\phi$$

and u_x , u_y , and u_z are components of a unit vector U which indicates the direction of the screw axis.

The rotation angle ϕ is found in the following manner:

$$\text{Trace} = a_{11} + a_{22} + a_{33} \quad (3.8)$$

where a_{ij} indicate entries in RM

$$\text{Trace} = u_x^2 V\phi + C\phi + u_y^2 V\phi + C\phi + u_z^2 V\phi + C\phi \quad (3.9)$$

$$= (u_x^2 + u_y^2 + u_z^2) (1 - \cos\phi) + 3 \cos\phi \quad (3.10)$$

Since \bar{U} is a unit vector

$$1 = u_x^2 + u_y^2 + u_z^2 \quad (3.11)$$

Combining (3.10) and (3.11)

$$\text{Trace} = 1 + 2 \cos\phi \quad (3.12)$$

$$\cos\phi = \frac{\text{Trace} - 1}{2} \quad (3.13)$$

$$\phi = \cos^{-1}$$

Once ϕ is calculated u_x , u_y , and u_z are determined.
Referring to equation (3.7).

$$a_{32} = u_y u_z V \phi + u_x S \phi \quad (3.15)$$

$$a_{23} = u_y u_z V \phi - u_x S \phi \quad (3.16)$$

$$a_{32} - a_{23} = 2 u_x S \phi \quad (3.17)$$

$$u_x = \frac{a_{32} - a_{23}}{2 S \phi} \quad (3.18)$$

By similar reasoning

$$u_y = \frac{a_{13} - a_{31}}{2 S \phi} \quad (3.19)$$

$$u_z = \frac{a_{21} - a_{12}}{2 S \phi} \quad (3.20)$$

Note that for this algorithm the values of u_x , u_y , and u_z are computed using the value of ϕ calculated in equation (3.14).

Now assume that two points, \bar{A} and \bar{B} , are on a rigid body. $\overline{AB1}$ is a vector from point \bar{A} to point \bar{B} when the rigid body is at position 1, and $\overline{AB2}$ is the same vector at rigid body position 2. Since \bar{A} and \bar{B} are on a rigid body the magnitude of \overline{AB} cannot change, but \overline{AB} will follow the rigid body rotation. From equation (3.3):

$$RM \quad \overline{AB1} = \overline{AB2} \quad (3.21)$$

or

$$RM \quad (\overline{B1} - \overline{A1}) = \overline{B2} - \overline{A2} \quad (3.22)$$

where:

$\overline{B1}$ is point \overline{B} when the rigid body is at position 1

$\overline{B2}$ is point \overline{B} when the rigid body is at position 2

Point \overline{A} has similar notation

\overline{A} , \overline{B} , \overline{AB} are not in homogeneous coordinates

Rearrange (3.22)

$$RM (\overline{B1} - \overline{A1}) + \overline{A2} = \overline{B2} \tag{3.23}$$

Equation (3.23) is a 3 x 3 system of equations. Add the equation $l=1$ to get:

$$\begin{bmatrix} B2_x \\ B2_y \\ B2_z \\ 1 \end{bmatrix} = \begin{bmatrix} RM & & & \\ & & & \\ & & & \\ 0 & 0 & 0 & 1 \end{bmatrix} \begin{bmatrix} \overline{A2} - RM \overline{A1} \\ \\ \\ 1 \end{bmatrix} \begin{bmatrix} B1_x \\ B1_y \\ B1_z \\ 1 \end{bmatrix} \tag{3.24}$$

The 4 x 4 matrix mapping $\overline{B1}$ to $\overline{B2}$ is DM. The elements of the fourth column of DM can be defined from equation (3.24).

$$a_{14} = A2_x - a_{11}A1_x - a_{12}A1_y - a_{13}A1_z \tag{3.25}$$

and so on.

$\overline{A1}$ is any arbitrary point on the same rigid body as \overline{B} .

Assume \bar{A} is on the screw axis so that it translates only, and rotations do not change the position of \bar{A} . Thus,

$$\bar{A}2 = \bar{A}2 + s \bar{U}.$$

Therefore:

$$a_{14} = su_x + Al_x - a_{11}Al_x - a_{12}Al_y - a_{13}Al_z \quad (3.26)$$

and so on for a_{24} and a_{34}

In matrix form:

$$\begin{bmatrix} a_{14} \\ a_{24} \\ a_{34} \end{bmatrix} = \begin{bmatrix} u_x (1-a_{11}) & -a_{12} & -a_{13} \\ u_y & -a_{21} & (1-a_{22}) & -a_{23} \\ u_z & -a_{31} & -a_{32} & (1-a_{33}) \end{bmatrix} \begin{bmatrix} s \\ Al_x \\ Al_y \\ Al_z \end{bmatrix} \quad (3.27)$$

The translation s , and Al_x , Al_y , and Al_z cannot be solved for because there are three equations and four unknowns. However, \bar{A} is of interest only because it fixes the screw axis in space. Thus any point on the screw axis will suffice. The point where the screw axis intersects a coordinate plane of the inertial axis system is called a piercing point. At a piercing point one of the coordinates is 0.0 depending on which plane is intersected. For example, the piercing point for the XY plane has a Z coordinate of 0.0. Setting one of the components of \bar{A} equal to 0.0, reduces equation (3.27) to three equations and three

unknowns, which yields \bar{A} and s .

Suh and Radcliffe's method [27] has been presented so far. Kinzel, et al. [13, 14] present a different algorithm. As part of this research Kinzel's methods were compared to Suh and Radcliffe's. In most cases both methods gave similar answers, but at not time did Kinzel's method give more accurate results, and on occasion Kinzel's method gave less accurate results. Suh and Radcliffe's method involves less computation, and is more straightforward.

One final note on the algorithm. In determining u_x , u_y , and u_z Suh and Radcliffe rely on the off diagonal elements of DM. These terms are very small for a small rotation, and they may be adversely effected by round off error. For this case one further method exists for finding \bar{U} . Recall equation (3.7).

$$a_{11} = u_x^2 v \phi + C \phi \quad (3.28)$$

$$a_{11} - C \phi = u_x^2 (1 - C \phi) \quad (3.29)$$

$$u_x^2 = \frac{a_{11} - C \phi}{1 - C \phi} \quad (3.30)$$

$$u_x = \sqrt{\frac{a_{11} - C \phi}{1 - C \phi}} \quad (3.31)$$

This method can be similarly applied for u_y and u_z . Note that in equation (3.31) the sign of u_x is not known. The sign must be determined using Suh and Radcliffe's

method, but the magnitude of u_x is found with equation (3.31). In the screw axis program implemented \bar{U} is found using equations (3.18-3.20). If the magnitude of U is not within some epsilon (± 0.01 in SAL) of 1, then equation (3.31) is used.

3.5 Relationship to the Eigenvalue Problem

If an eigen analysis is done on RM there will be one real eigenvalue, and one pair of complex conjugate eigenvalues. The imaginary part of the complex eigenvalue is the rotation angle ϕ in radians. The one real eigenvector will be a vector in the direction of the screw axis. Because of the different algorithms used to compute eigenvectors, the eigenvector may not have a unit magnitude, but a simple scaling of the eigenvector will give \bar{U} . The real eigenvalue also gives a method of determining if RM is orthogonal. If the real eigenvalue does not equal 1, RM is not orthogonal. In computer graphics, if the size of an object is to be enlarged or shrunk, the eigenvalue represents the magnification factor. Orthogonal transformations preserve lengths and thus have eigenvalues (magnification factors) of 1. The real eigenvalue of RM provides information on how much the lengths between the data points changed between position 1 and position 2.

CHAPTER 4

THREE DIMENSIONAL POSITION DESCRIPTION

4.1 Introduction

As discussed in Section 3.3, "Computation of DM from Position Data", only three non-collinear points are needed to describe the position of a rigid body in space. Two algorithms for computing DM from position data were presented, namely, 1) a fourth point may be created by rotating the third data point about an axis between the first two data points, or 2) a coordinate system based on the three data points is set up, and three new points at unit distances from the created origin, one on each axis, together with the origin make up the four points.

If the first method, rotating the third point, is used, the three points must maintain their position relative to one another, from one position of the rigid body to another. Any change in the true relative position of the points, or an apparent change due to measurement error, violates the rigid body assumption. Violating the rigid body assumption results in a non-orthogonal RM. The effect of measurement error is an apparent shrinking or stretching of the rigid body. DM reflects this change in size even though the object has not changed. Numerical problems may

result. For example, in the determination of ϕ through equation (3.14) it may be necessary to find the inverse cosine of a number greater than 1. Or the computed magnitude of \bar{U} may deviate from 1. Different values of s , the translation parallel to the screw axis, may result from using different piercing points.

Early in the work for this thesis the possibility was investigated that scaling the magnitudes of the columns of RM to 1.0 would avoid a non-orthogonal RM. This did not work because scaling simply changes the magnitudes of the entries in RM. The reason RM is not orthogonal is that the ratios within the rows and columns of RM are incorrect.

The second method of computing DM from position data, setting up a coordinate system based on the three data points, prevents measurement errors from propagating through the analysis. An algorithm for setting up a coordinate system is presented in the next section. The coordinate system approach always gives an orthogonal RM since the coordinate systems rather than the measured data are used to compute DM. Each point used is always a unit distance away from the origin. Further, since the coordinate system set up has three mutually perpendicular axes, the system is already orthogonal. This does not mean the method is error free. An error in any of the data points used to create the new coordinate system will change the location and orientation of the new axis system.

4.2 Algorithm for Setting Up a Coordinate System Based on Three Data Points

Three points define a plane, and in the problem at hand the three points define one of the coordinate planes. Call the data points \bar{A} , \bar{B} , and \bar{C} . Create vectors from \bar{A} to \bar{B} (\overline{AB}), and from \bar{A} to \bar{C} (\overline{AC}). This is done by subtracting components.

$$\begin{aligned}\overline{AB} &= \text{vector from A to B} \\ &= (B_x - A_x) i + (B_y - A_y) j + (B_z - A_z) k \quad (4.1) \\ &\text{where } i, j, k \text{ are unit coordinate vectors} \\ \overline{AC} &\text{ is similarly defined}\end{aligned}$$

The dot product of the two vectors AB and AC is defined by

$$\overline{AB} \cdot \overline{AC} = AB_x AC_x + AB_y AC_y + AB_z AC_z = |\overline{AB}| |\overline{AC}| \cos \theta \quad (4.2)$$

Rearrange (4.2) to get:

$$\cos \theta = \frac{\overline{AB} \cdot \overline{AC}}{|\overline{AB}| |\overline{AC}|} \quad (4.3)$$

The origin of the new coordinate system is a point on \overline{AB} which lies on a line perpendicular to \overline{AB} and containing \bar{C} . The distance along \overline{AB} from \bar{A} to the new origin (\overline{Or}) is $|\overline{AC}| \cos \theta$. Thus the three dimensional coordinates of the origin are determined from:

OB and OC are unit vectors created.
OB x OC comes out of the Page
A, B, C are Anatomical Data Points

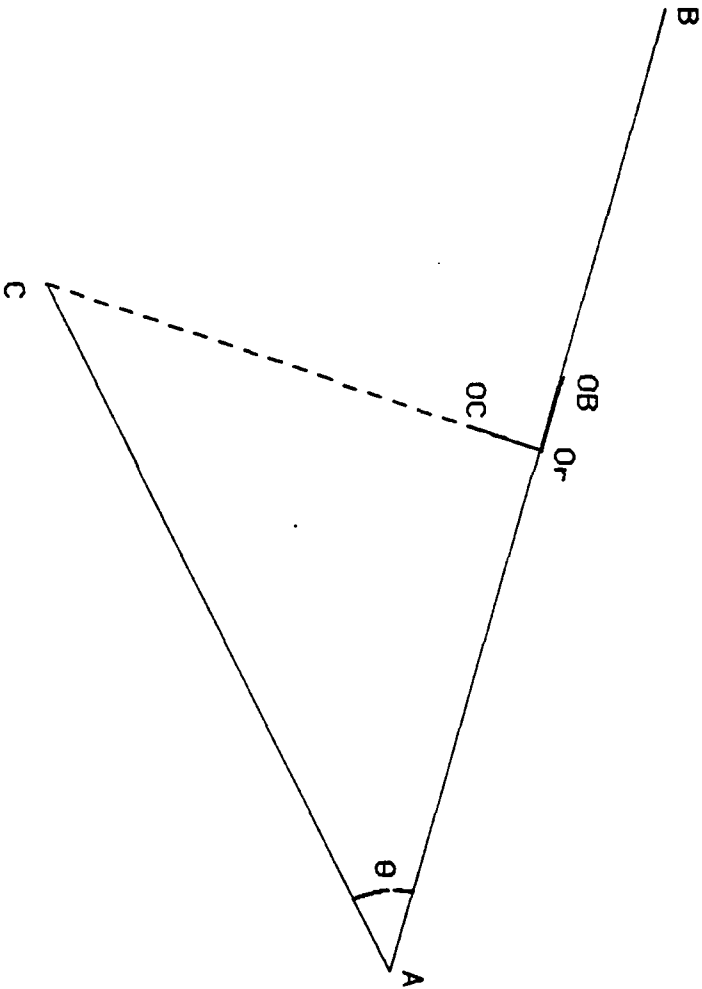


Figure 4-1 Data Based Coordinate System

$$\overline{Or} = \overline{A} + \frac{\overline{AB}}{|\overline{AB}|} |\overline{AC}| \cos\theta \quad (4.4)$$

Vector \overline{AB} is divided by its magnitude to form a unit vector in the direction of \overline{AB} . Once the origin's coordinates (\overline{Or}) are established with equation (4.4) unit vectors in the direction from \overline{Or} to \overline{B} (\overline{OB}), and from \overline{Or} to \overline{C} (\overline{OC}) are determined. These unit vectors are then added to \overline{Or} to determine the location of a point on each axis. Finally, the vector cross product of the unit vectors \overline{OB} and \overline{OC} determines the direction of the third axis. Four points have been created, \overline{Or} , and the end points of unit vectors \overline{OB} , \overline{OC} , and $\overline{OB} \times \overline{OC}$. These four new points may now be used to directly solve for DM.

4.3 Effect of Errors on Coordinate System Determination

The effect of an error in a data point used to define a coordinate system has been analyzed by Robbins 24 . The analysis which follows uses a different technique but similar conclusions are reached. Recall equation (4.2).

$$|\overline{AB}| |\overline{AC}| \cos\theta = AB_x AC_x + AB_y AC_y + AB_z AC_z \quad (4.5)$$

The effect of an error, dx , in the x coordinate of point \overline{B} can be evaluated using the partial derivative with respect to x [2] of equation (4.5).

$$|\overline{AB}| |\overline{AC}| d\theta \sin \theta = AC_x dx \quad (4.6)$$

$$d\theta = \frac{AC_x dx}{|\overline{AB}| |\overline{AC}| \sin \theta} \quad (4.7)$$

If the angle θ between \overline{AB} and \overline{AC} is small then $\sin \theta$ will be small, and the error propagation will become large.

$$\lim_{\theta \rightarrow 0} d\theta = \lim_{\theta \rightarrow 0} \frac{AC_x dx}{|\overline{AB}| |\overline{AC}| \sin \theta} = \infty \quad (4.8)$$

In addition, the closer point \overline{B} is to point \overline{A} , the smaller the magnitude of \overline{AB} .

$$\lim_{|\overline{AB}| \rightarrow 0} d\theta = \lim_{|\overline{AB}| \rightarrow 0} \frac{AC_x dx}{|\overline{AB}| |\overline{AC}| \sin \theta} = \infty \quad (4.9)$$

Equations (4.8) and (4.9) show that the angle between \overline{AB} and \overline{AC} should be as close to 90° as possible, and points \overline{B} and \overline{C} should be located as far away from point \overline{A} as possible. At present the computer program which creates the coordinate system for use in the screw axis analysis, does not check for either of these conditions, and this is an area worthy of further investigation in SAL.

CHAPTER 5
ERROR ANALYSIS

5.1 How Errors in Position Effect the DM

The propagation of measurement errors through the matrix operations used to compute DM is a complicated question to analyze. This section develops a method of bounding this error propagation based on methods used in numerical analysis. It is not within the scope of this thesis to provide a full and complete analysis of matrix propagation of measurement error. Rather, this thesis provides an introduction to this subject. Recall equation (3.6):

$$DM = P_2 P_1^{-1} \quad (3.6)$$

The error in P_1^{-1} is difficult to evaluate because each element of P_1^{-1} is a function of several elements of P_1 . In addition, the elements of P_1 which determine an element of P_1^{-1} are different for each element of P_1^{-1} .

The field of numerical analysis has dealt with the question of how error in a matrix effects the inverse. Round off error in a computer has an effect similar to measurement error in empirical data. To analyze the effect of round off error, Forsythe and Moler [11] define a number

called the condition number. Assume a system of linear equations exists,

$$A x = b \quad (5.1)$$

where:

A is a known $n \times n$ matrix

x is an unknown n vector, or an unknown matrix, and is to be solved for

b is a known n vector, or a known matrix

By definition:

$$\text{condition number} = \text{cond}(A) = \frac{\|A\|}{\|A^{-1}\|} \quad (5.2)$$

where $\|A\|$ is the euclidean norm of the matrix A. For an $n \times n$ matrix A, the euclidean norm is

$$\sqrt{\sum_{i=1}^n \sum_{j=1}^n a_{ij}^2} \quad (5.3)$$

The condition number will never be less than 1, but it may approach infinity. The greater $\text{cond}(A)$, the greater the error propagation in the resulting inverse and/or solution to a set of linear equations.

As an example of equations (5.1-5.3), assume

$$A = \begin{bmatrix} 1 & 4 \\ 3 & 5 \end{bmatrix}$$

so

$$A^{-1} = -\frac{1}{7} \begin{bmatrix} 5 & -4 \\ -3 & 1 \end{bmatrix}$$

From equation (5.2)

$$A = \sqrt{(1)^2 + (3)^2 + (4)^2 + (5)^2} = 7.14$$

and

$$A^{-1} = \sqrt{(1/7)^2 + (5)^2 + (-3)^2 + (-4)^2 + (1)^2} = 1.02$$

Using equation (5.2)

$$\text{cond}(A) = (7.14) (1.02) = 7.28$$

Forsythe and Moler [11] state that for a system of equations such as equation (5.1).

$$\frac{\| \overset{\Delta}{x} \|}{\| x \|} \leq \text{cond}(A) \frac{\| e_b \|}{\| b \|} \quad (5.4)$$

where:

e_x is a matrix containing the errors in the solution x

e_b is a matrix containing the errors in matrix b

In similar fashion, an error in A, e_A , produces an error in x bounded by

$$\frac{\|e_x\|}{\|x + e_x\|} \leq \text{cond}(A) \frac{\|e_A\|}{\|A\|} \quad (5.5)$$

Assume that e_x is insignificant compared to x , then equation (5.5) becomes

$$\frac{\|e_x\|}{\|x\|} \leq \text{cond}(A) \frac{\|e_A\|}{\|A\|} \quad (5.6)$$

Assume the worst case in equation (5.4) and (5.6) so that the inequality is replaced by an equality.

Define e_{xb} as a matrix containing the error in the solution due to errors in b , and define e_{xA} as a matrix containing the error in a solution due to errors in A . Combine equations (5.4) and (5.6)

$$\frac{\|e_{xA}\|}{\|x\|} + \frac{\|e_{xb}\|}{\|x\|} = \text{cond}(A) \frac{\|e_A\|}{\|A\|} + \text{cond}(A) \frac{\|e_b\|}{\|b\|} \quad (5.7)$$

Define $e_x = e_{xA} + e_{xb}$

$$\|e_x\| = \|x\| \text{cond}(A) \left(\frac{\|e_A\|}{\|A\|} + \frac{\|e_b\|}{\|b\|} \right) \quad (5.8)$$

To continue the previous example assume A and b consist of measurements with a measurement error of $\pm .01$.

Then,

$$e_A = e_b = \begin{bmatrix} .01 & .01 \\ .01 & .01 \end{bmatrix}$$

Use equation (5.2) to find

$$|| e_A || = || e_b || = .01 \sqrt{4} = .02$$

Assume

$$b = \begin{bmatrix} 1.5 & 4.25 \\ 2.5 & 5.6 \end{bmatrix}$$

and

$$|| b || = \sqrt{(1.5)^2 + (2.5)^2 + (4.25)^2 + (5.6)^2} = 7.61$$

Equation (5.1) may be solved by inverting A and multiplying the inverse times b.

$$x = A^{-1} b$$

$$x = \begin{bmatrix} -5/7 & 4/7 \\ 3/7 & -1/7 \end{bmatrix} \begin{bmatrix} 1.5 & 4.25 \\ 2.5 & 5.6 \end{bmatrix}$$

$$= \begin{bmatrix} .357 & .164 \\ .286 & 1.02 \end{bmatrix}$$

and using equation (5.3)

$$||x|| = \sqrt{(3.57)^2 + (.286)^2 + (.164)^2 + (1.02)^2} = 1.13$$

Substitute into equation (5.8)

$$\begin{aligned} ||e_x|| &= (1.13) (7.28) \left(\frac{.02}{7.14} + \frac{.02}{7.61} \right) \\ &= 0.45 \end{aligned}$$

In computing DM, A is P1, b is P2, and x is DM. Substitute into equation (5.8) to get

$$||e_{DM}|| = ||DM|| \text{ cond}(A) \left(\frac{||e_{P1}|| + ||e_{P2}||}{||P1|| \quad ||P2||} \right) \quad (5.9)$$

5.2 How Errors in DM Effect the Screw Axis

In determining the screw axis parameters the opportunity for error to multiply is enhanced by the fact that \bar{U} is determined from ϕ , which may already be in error, and s is determined from \bar{U} . In this section it will be shown that an error in the angle of rotation may be very large, and yet that rotation angle is needed to determine directly, or indirectly, all other screw axis parameters. Recall from Chapter 3 that the first step in finding the screw axis parameters is to find ϕ using equation (3.14).

$$\phi = \cos^{-1} \left(\frac{\text{Trace} - 1}{2} \right) \quad (5.10)$$

The trace is the sum of the diagonal elements of RM. If each element is in error by an equal amount e_{DM} , the trace will be in error by the following

$$e_{TR} = e_{DM} \sqrt{3} \quad (5.11)$$

This is derived by setting the resulting error equal to the square root of the sum of the individual errors {2}. As an example assume $e_{DM} = \pm .0008$, then $e_{TR} = \pm .00138$.

Propogation of errors in the inverse cosine is calculated by taking the derivative of the function {2}:

$$\phi = \cos^{-1} x \quad (5.12)$$

$$d\phi = \frac{dx}{\sqrt{1-x^2}} \quad (5.13)$$

$$\text{where: } x = \frac{\text{Trace} - 1}{2}$$

Figure 5-1 presents the error in the rotation angle resulting from $e_{TR} = .00138$. The figure indicates that the error term is significant for small angles. For example, if the correct value of ϕ is 0.8° the induced error is 5.6° . Further calculations using equation (5.13) show that if rotation angles on the order of 1° are to be measured to within $\pm 0.5^\circ$, the required accuracy in the Trace is $\pm .0003$, or e_{DM} must be less than .00018.

Note that e_{TR} for Figure 5-1 is .00138 indicating only

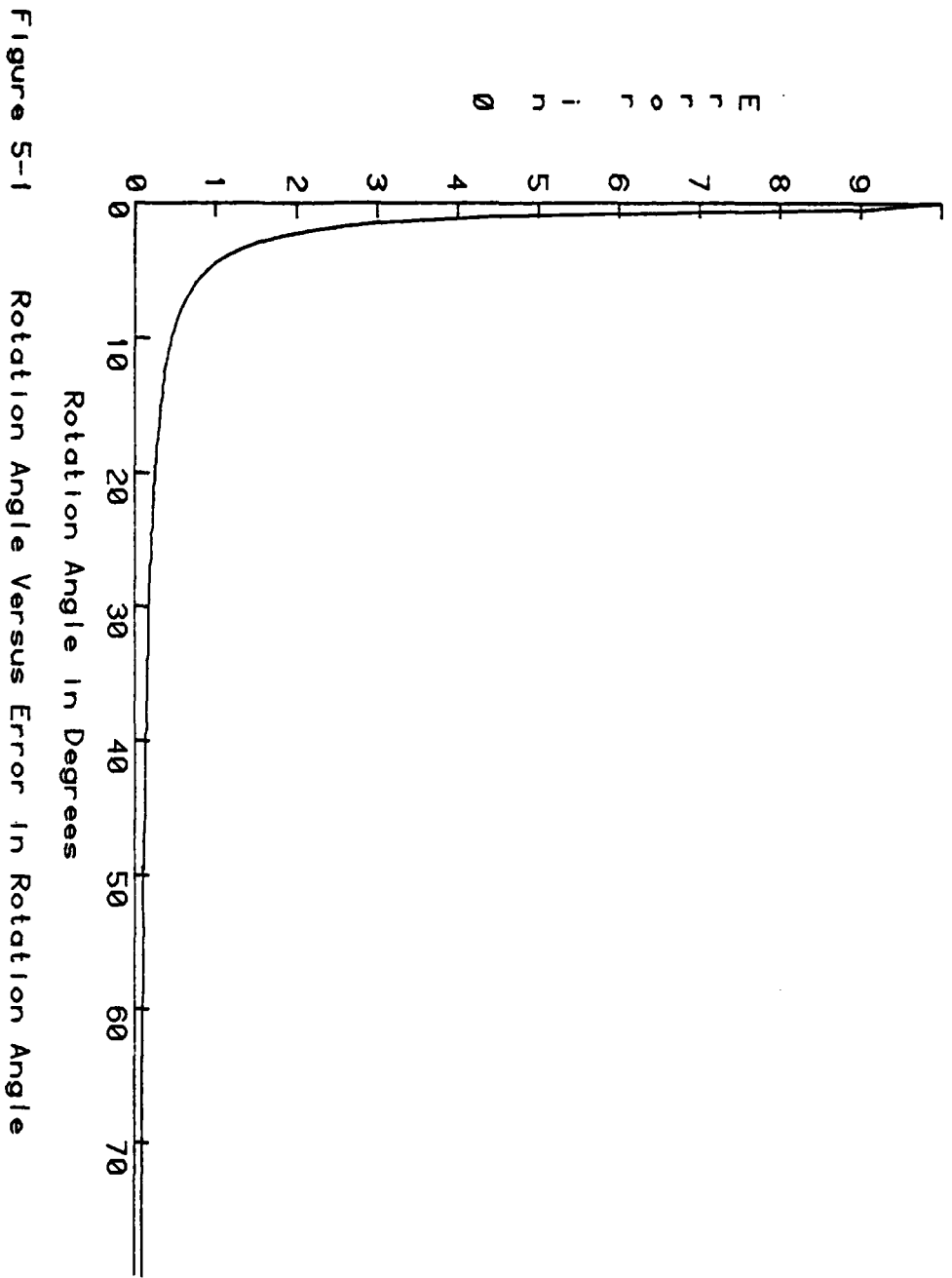


Figure 5-1 Rotation Angle Versus Error in Rotation Angle

E R R O R

three significant figures are available. The number of significant figures which can be used in calculations has an effect on the accuracy of ϕ . Table 5-1 illustrates the effect of significant figures when ϕ is small.

Table 5-1 was computed in the following manner. If $\cos \phi$ has two significant figures that means the value is between .9949 and .985. The inverse cosine of .9949 is 5.73° . The inverse cosine of .985 is 9.94° . The resolution is $9.94^\circ - 5.73^\circ$, or 4.21° .

TABLE 5-1

Effect of Significant Figures on Small Angles

<u>Significant Figures</u>	<u>Cos ϕ</u>	<u>Resolution</u>
2	.99	4.21
3	.999	1.33
4	.9999	0.42
5	.99999	0.13
6	.999999	0.04
7	.9999999	0.01

Because at small angles, sine is less affected by an error than cosine, the possibility of using the sine to find ϕ was investigated. Two different methods exist for using the sine, but neither is more accurate than using the cosine. The first method investigated involves substituting $1 - \sin^2 \phi$ for $\cos^2 \phi$, and the second method utilizes the off diagonal elements of RM. Changing the names of variables does not avoid the basic cause of the error propagation. To measure small rotation angles on the order of 1° accurate

measurements of rigid body positions are needed, and as many significant figures as possible should be retained. To find ϕ to $\pm .13^\circ$ when the rotation angle is 1° requires that five significant figures be available for computations.

Once ϕ is known the components of \bar{U} , the unit vector in the direction of the screw axis, are computed using equations (3.18-3.20). Consider the computation of u_x

$$u_x = \frac{a_{32} - a_{23}}{2 \sin \phi} \quad (3.18)$$

To find the effect of an error, take the partial derivatives {2}, one with respect to ϕ , and one with respect to $(a_{32} - a_{23})$

$$du_x = \frac{\cos \phi \, d(a_{32} - a_{23})}{2 \sin^2 \phi} + \frac{d(a_{32} - a_{23})}{2 \sin \phi} \quad (5.14)$$

It may be argued that a_{32} and a_{23} are functions of ϕ (see equation 3.2 for the proof of this) and should have been differentiated with respect to ϕ . An error in ϕ arises from errors defined in equation (5.13) which is independent of a_{32} and a_{23} . The values of a_{32} and a_{23} arise from the computation of DM, and an error in the calculated value of ϕ will not effect a_{32} and a_{23} .

Equation (5.14) reveals that even if ϕ is known exactly, i.e. $d\phi = 0$, error in DM may still propagate into

the value of \bar{U} . Error in $(a_{32} - a_{23})$ is related to the error in DM, and that error is multiplied by $\frac{1}{\sin^2 \phi}$. If ϕ is small, $\frac{1}{\sin \phi}$ is large, independent of $d\phi$. In addition to measurement error in DM, when ϕ is small RM approaches an identity matrix causing off diagonal elements such as a_{32} and a_{23} to be effected by round off error.

An error in $(a_{32} - a_{23})$ is defined by finding the square root of the sum of the individual errors squared {2}.

$$d(a_{32} - a_{23}) = \sqrt{e_{32}^2 + e_{23}^2} \quad (5.15)$$

As an example of the error progation in finding u_x , assume

$$\begin{aligned} \phi &= 1^\circ \text{ (.0174 rad)} \\ d\phi &= 0.25^\circ \text{ (.004 rad)} \\ (a_{32} - a_{23}) &= .001 \\ e_{32} = e_{23} &= .0008 \end{aligned}$$

By equation (5.15)

$$d(a_{32} - a_{23}) = .0008 \sqrt{2} = .0011$$

To find the error in u_x use equation (5.14)

$$\begin{aligned} du_x &= \frac{(.999) (.004) (.0010)}{2(.0174)^2} + \frac{.0011}{2(.0174)} \\ &= .038 \end{aligned}$$

The error in u_x will be increased compared to the error in DM when ϕ is small, even though ϕ may be known exactly. As with the determination of ϕ , small angles require accuracy and precision to determine \bar{U} .

The final step in the screw axis algorithm is to solve for the translation s , and a piercing point \bar{A} . As in finding DM this is a matrix operation. Recall equation (3.27)

$$\begin{bmatrix} a_{14} \\ a_{24} \\ a_{34} \end{bmatrix} = \begin{bmatrix} u_x & (1-a_{11}) & -a_{12} & -a_{13} \\ u_y & -a_{21} & (1-a_{22}) & -a_{23} \\ u_z & -a_{31} & -a_{32} & (1-a_{33}) \end{bmatrix} \begin{bmatrix} s \\ A_x \\ A_y \\ A_z \end{bmatrix} \quad (3.27)$$

Assume $A_z = 0.0$, i.e., the piercing point lies in the XY plane

$$\begin{bmatrix} a_{14} \\ a_{24} \\ a_{34} \end{bmatrix} = \begin{bmatrix} u_x & (1-a_{11}) & a_{12} \\ u_y & a_{21} & (1-a_{22}) \\ u_z & a_{31} & a_{32} \end{bmatrix} \begin{bmatrix} s \\ A_x \\ A_y \end{bmatrix} \quad (5.16)$$

$$\text{Set } b = \begin{bmatrix} a_{14} \\ a_{24} \\ a_{34} \end{bmatrix} \quad A = \begin{bmatrix} u_x & (1-a_{11}) & -a_{12} \\ u_y & -a_{21} & (1-a_{22}) \\ u_z & -a_{31} & -a_{32} \end{bmatrix} \quad x = \begin{bmatrix} s \\ A_x \\ A_y \end{bmatrix}$$

A and b are known to within a certain error. The error in x is bounded by equation (5.8)

$$\|e_x\| = \|x\| \operatorname{cond}(A) \left(\frac{\|e_A\|}{\|A\|} + \frac{\|e_b\|}{\|b\|} \right) \quad (5.8)$$

5.3 Conclusion

In this theoretical error analysis the difficult question of error propagation through matrix operations has been evaluated using methods from numerical analysis. Within a given accuracy in DM the screw axis analysis is particularly sensitive to small rotation angles. This sensitivity cannot be reduced by using $\sin \phi$ instead of $\cos \phi$. The limit of accuracy in determining \bar{U} is the size of ϕ . To find values of ϕ on the order of 1° to within $\pm .5^\circ$ requires that the accuracy of DM be better than $\pm .0002$, and that all four significant figures be retained. The next chapter shows how the addition of error to "perfect data" actually changes the screw axis parameters.

CHAPTER 6

EVALUATION OF THE ACTUAL EFFECT OF ADDING ERRORS

6.1 Introduction and Description of Procedure

The results of Chapter 5 indicate that screw axis analysis is inaccurate for small rotation angles. To gain insight into how an actual error in the position data effects the entire screw axis algorithm, including coordinate system determination and computation of DM, "perfect" error free position measurements were computed. Selected errors were then added to the measurements and the effect on the screw axis was evaluated. The data were created with a set of points in a geometrical arrangement, and at distances (in cm) typical of targets on a human femur. The "perfect" data is created by specifying:

- 1) The number of significant digits in the position measurements
- 2) A point in space which fixes the screw axis
- 3) Three components of a unit vector in the direction of the screw axis
- 4) A rotation around the screw axis
- 5) A translation parallel to the screw axis

The data points created are then used in a computer

program which preforms a screw axis analysis, prints out the results, and then adds an error of +.10 cm to a single data coordinate. The analysis then starts over again, including the creation of the coordinate system at each position. This is followed by removing the error added in the previous step, and then adding an error of +.10 cm to another data coordinate. This process is repeated until all 18 coordinates specifying two rigid body positions have been perturbed.

To simulate the effect of random error, it is also possible to add different random errors to each coordinate of the "perfect" position measurements. This is accomplished by specifying:

- 1) The number of significant digits
- 2) A scale factor bounding the random error. If a digitizer accurate to ± 0.01 cm is to be modeled, the scale factor would be .01

The results of this error adding routine are then passed to the screw axis analysis program. In this manner the effect of random errors in position data is evaluated.

6.2 Results

In view of the sensitivity of screw axis analysis to small rotation angles ϕ , a number of different rotation angles were analyzed. The rotations were varied from 1° to 60° . In each case the screw axis was the same, both in location and direction. The translation s was specified as 0.0 in order to see how s varied positively and negatively.

TABLE 6-1 Error With $\phi = 1.0^\circ$; 4 Significant Figures

(Note: In Perturbation Column, +.1x indicates that 0.1cm was added to the x coordinate

		Piercing Point = 0, 10, 0				U = .57735, -.57735, .57735				$\phi = 1.0^\circ$			
Perturbation	UX	UY	UZ	$\phi(\text{deg})$	s	Alx	AlY	Alz	Cond(P1)	P1	P2		
None (No error)	.604	-.587	.54	.986	.01	-.48	10.2	0	4081	76.81	77.04		
Position 1													
+ .1x Point 1	.549	-.667	.501	1.082	-.06	0	8.74	-3.69	4076	76.80	77.04		
+ .1y	.678	-.532	.514	1.088	.08	0	9.26	-4.49	4080	76.85	77.04		
+ .1z	.595	-.602	.533	1.002	0	0	9.49	-0.30	4080	76.81	77.04		
Position 2													
+ .1x Point 2	.357	-.331	.875	1.344	-.04	0	7.05	-3.03	4082	76.82	77.04		
+ .1y	.476	-.625	.615	.928	-.02	1.54	11.36	0	4077	76.77	77.04		
+ .1z	.558	-.540	.626	1.028	0	0	9.43	-0.37	4081	76.81	77.04		
+ .1x Point 3	.773	-.618	-.0131	.920	.07	0	5.95	4.47	4085	76.84	77.04		
+ .1y	.633	-.602	.486	.96	.01	0	9.76	0.94	--	--	--		
Position 2													
+ .1x Point 1	.660	-.481	.576	.907	.08	0	11.86	3.85					
+ .1y	.507	-.647	.566	.894	-.08	0	8.94	6.19					
+ .1z	.614	-.572	.549	.966	.02	0	10.03	1.24					
Position 2													
+ .1x Point 2	.700	-.703	-.108	1.013	.06	0	7.85	4.79					
+ .1y	.703	-.542	.459	1.066	.03	0	7.04	1.43					
+ .1z	.646	-.629	.432	.959	.02	0	9.84	1.34					
+ .1x Point 3	.341	-.418	.842	1.405	-.05	0	8.42	-4.1					
+ .1y	.571	-.568	.592	1.020	0	0	9.72	-0.14					
+.05 random													
+ .01 random	.808	-.591	0	.908	.10	0	6.54	5.68					
+ .1 random	.62	-.587	.53	.966	.02	0	9.17	2.16					
+ .1 random	.773	-.542	-.342	1.148	.19	0	10.04	4.37					

TABLE 6-2 Error With $\phi=10$; 5 Significant Figures

(Note: In Perturbation Column, +.1x indicates that 0.1cm was added to the x coordinate

Piercing Point = 0, 10, 0

U = .57735, -.57735, .57735

$\phi = 1.00$

Perturbation	UX	UY	UZ	ϕ (deg)	s	Alx	Alx	Alz	Cond(P1)	P1	P2
None (No error)	.577	-.577	.577	1.003	0	0	9.96	-.01	4080	76.8	77.03
Position 1											
+ .1x Point 1	.527	-.658	.533	1.095	-.06	0	8.86	-4.12	4075	76.8	77.03
+ .1y	.655	-.525	.546	1.10	.07	0	9.65	-4.93	4079	76.84	77.03
+ .1z	.569	-.592	.566	1.018	-.01	0	9.69	-0.74	--	--	--
+ .1x Point 2	.337	-.323	.885	1.376	-.04	0	7.06	-3.42			
+ .1y	.451	-.614	.649	.943	-.03	0	13.55	-2.74			
+ .1z	.536	-.533	.659	1.041	-.01	0	9.57	-0.81			
+ .1x Point 3	.768	-.628	-.086	.905	.07	0	6.58	4.44			
+ .1y	.608	-.594	.523	.972	.01	0	10.04	0.51			
Position 2											
+ .1x Point 1	.629	-.471	.610	.925	.08	0	12.25	3.40			
+ .1y	.479	-.633	.60	.913	-.08	0	8.79	5.89			
+ .1z	.588	-.563	.583	.981	.01	0	10.28	.80			
+ .1x Point 2	.693	-.712	-.067	.999	.06	0	8.5	4.7			
+ .1y	.681	-.537	.493	1.076	.02	0	7.31	1.18			
+ .1z	.622	-.621	.470	.970	.01	0	10.17	0.92			
+ .1x Point 3	.323	-.409	.852	1.436	-.06	0	8.44	-4.57			
+ .1y	.545	-.558	.622	1.038	-.01	0	9.9	-0.59			

TABLE 6-3 Error With $\phi = 5^\circ$; 4 Significant Figures

(Note: In Perturbation Column, +.1x indicates that 0.1cm was added to the x coordinate)
 Piercing Point = 0, 10, 0

J = .57735, -.57735, .57735
 $\phi = 5.0^\circ$

Perturbation	<u>UX</u>	<u>UY</u>	<u>UZ</u>	ϕ (deg)	<u>s</u>	<u>Alx</u>	<u>Alx</u>	<u>Alx</u>	<u>Alz</u>
None (No error)	.581	-.577	.574	4.99	.01	0	0	9.89	.09
<u>Position 1</u>									
+ .1x Point 1	.571	-.595	.565	5.08	-.06	0	0	9.61	-0.74
+ .1y	.597	-.566	.569	5.09	.08	0	0	9.89	-0.99
+ .1z	.579	-.581	.573	5.01	0	0	0	9.84	-0.06
+ .1x Point 2	.527	-.526	.668	5.25	-.05	0	0	9.45	-.84
+ .1y	.557	-.586	.589	4.93	-.02	0	0	10.51	-.27
+ .1z	.571	-.569	.592	5.03	0	0	0	9.83	-.08
+ .1x Point 3	.642	-.606	.470	4.72	.08	0	0	9.80	1.18
+ .1y	.587	-.581	.564	4.96	.01	0	0	9.90	0.19
<u>Position 2</u>									
+ .1x Point 1	.564	-.589	.580	4.89	-.07	0	0	9.78	1.23
+ .1y	.582	-.574	.576	4.96	.02	0	0	9.95	0.33
+ .1z	.628	-.624	.464	4.80	.07	0	0	10.15	1.08
+ .1x Point 2	.594	-.588	.55	4.95	.02	0	0	9.92	0.33
+ .1y	.520	-.545	.657	5.33	-.06	0	0	9.82	-0.98
+ .1z	.572	-.573	.587	5.04	-.01	0	0	9.94	-0.08
+ .05 Random	.547	-.568	.615	5.13	-.05	0	0	9.44	0.35
+ .01 Random	.572	-.569	.591	5.05	0	0	0	9.79	-.07
+ .10 Random	.607	-.607	.513	5.07	.07	0	0	8.97	0.69

TABLE 6-4 Error With $\phi=10^\circ$; 4 Significant Figures
 (Note: In Perturbation Column, +.1x indicates that 0.1cm was added to the x coordinate)
 Piercing Point = 0, 10, 0
 $U = .57735, -.57735, .57735$
 $\phi = 10.0^\circ$

Perturbation	<u>UX</u>	<u>UY</u>	<u>UZ</u>	<u>ϕ(deg)</u>	<u>s</u>	<u>Alx</u>	<u>Alv</u>	<u>Alz</u>
None (No error)	.58	-.578	.574	9.99	0	0	9.93	.03
<u>Position 1</u>								
+ .1x Point 1	.575	-.587	.569	10.08	-.06	0	9.81	-.39
+ .1y	.588	-.572	.572	10.09	.08	0	9.99	-.52
+ .1z	.579	-.580	.573	10.01	-.01	0	9.91	-.04
<u>Position 2</u>								
+ .1x Point 2	.551	-.555	.623	10.23	-.05	0	9.76	-.47
+ .1y	.568	-.583	.581	9.93	-.02	0	10.23	-.13
+ .1z	.575	-.574	.583	10.03	-.01	0	9.9	-.06
<u>Position 3</u>								
+ .1x Point 3	.612	-.591	.525	9.7	.07	0	9.89	.59
+ .1y	.583	-.580	.569	9.6	.01	0	9.93	.09
<u>Position 2</u>								
+ .1x Point 1	.585	-.569	.578	9.92	.08	0	10.06	.38
+ .1y	.572	-.584	.577	9.89	-.07	0	9.86	.62
+ .1z	.680	-.576	.575	9.96	.01	0	9.96	.21
<u>Position 2</u>								
+ .1x Point 2	.605	-.600	.522	9.78	.06	0	10.08	.52
+ .1y	.593	-.575	.563	10.04	.03	0	9.64	.22
+ .1z	.589	-.584	.559	9.94	.02	0	9.94	.19
<u>Position 3</u>								
+ .1x Point 3	.549	-.565	.617	10.31	-.07	0	9.98	-.52
+ .1y	.574	-.576	.582	10.05	-.01	0	10.00	-.09
+ .05 Random	.602	-.590	.539	9.86	.03	0	10.09	.30
+ .10 Random	.574	-.577	.581	10.11	-.02	0	9.28	.08

TABLE 6-5 Error With $\phi=60^\circ$; 4 Significant Figures

(Note: In Perturbation Column, +.1x indicates that 0.1cm was added to the x coordinate)
 Piercing Point = 0, 10, 0
 $U = .57735, -.57735, .57735$
 $\phi = 60.00^\circ$

Perturbation	UX	UY	UZ	ϕ (deg)	s	ALx	ALy	ALz	Cond(P1)	P1	P2
None (No error)	.578	-.577	.577	60.0	.01	0	9.99	0	4081.	76.81	91.32
Position 1											
+ .1x Point 1	.578	-.579	.576	60.1	-.06	0	10.01	-.09	4076	76.81	91.32
+ .1y	.579	-.576	.577	60.1	.08	0	10.04	-.10			
+ .1z	.578	-.577	.577	60.1	0	0	9.99	-.01			
+ .1x Point 2	.570	-.577	.585	60.2	-.05	.11	9.90	0.0			
+ .1y	.576	-.579	.578	59.9	-.02	0	10.04	0.0			
+ .1z	.576	-.577	.578	60.0	0	0	9.99	-.02			
+ .1x Point 3	.585	-.576	.571	59.7	.08	0	9.94	0.11			
+ .1y	.579	-.577	.576	60.0	.01	0	9.98	0.01			
Position 2											
+ .1x Point 1	.579	-.575	.578	60.0	.10	0	10.01	-.01			
+ .1y	.577	-.578	.577	59.9	-.03	0	9.95	.09			
+ .1z	.577	-.577	.578	59.9	.03	0	9.95	0.11			
+ .1x Point 2	.581	-.578	.573	59.8	.03	0	10.00	0.07			
+ .1y	.581	-.576	.575	60.0	.04	0	9.95	0.03			
+ .05 random	.578	-.576	.578	60.0	.09	0	10.05	-.02			
+ .01 random	.577	-.577	.578	60.0	.02	0	9.99	.01			
+ .1 random	.597	-.578	.557	59.4	.20	0	9.82	0.26			

TABLE 6-6 Summary of Error Analysis

(Does not include random error cases analyzed)

For all cases Piercing Point = 0, 10., 0
 $U = .57735, -.57735, .57735$

Table	Input ϕ	Significant Figures	u _x		u _y		u _z		Computed ϕ		S	
			Max	Min	Max	Min	Max	Min	Max	Min	Max	Min
6-1	10	4	.773	.341	-.703	-.331	.875	-.108	1.405	.894	.08	-.08
6-2	10	5	.768	.337	-.712	-.323	.885	-.067	1.436	.905	.08	-.08
6-3	50	4	.642	.520	-.624	-.526	.668	.464	5.33	4.72	.08	-.07
6-4	100	4	.612	.549	-.600	-.555	.623	.522	10.31	9.60	.08	-.07
6-5	600	4	.585	.570	-.579	-.575	.585	.571	60.1	59.7	.10	-.06

Tables 6-1 through 6-5 display the results. In addition to perturbing each coordinate by $+ .10$ cm, three random error cases were analyzed. The digitizer used in SAL is accurate to $\pm .013$ cm, thus the first random error case was $\pm .01$. The second and third random cases are of $\pm .05$ cm and $\pm .10$ cm. Table 6-6 summarizes the five Tables preceding it, but the random error cases are not included. The inputs and the maximum and minimum values of the screw axis parameters are detailed in Table 6-6.

6.3 Discussion

Tables 6-1 and 6-2 show that small angles were computed more accurately than Chapter 5 would have indicated. For rotations as small as 1° the range of calculated values for ϕ was $\pm .41^\circ$, $-.11^\circ$. It is interesting to note that increasing the number of significant digits did not decrease the affect of an error. It should be kept in mind however, that the error added was $.10$ cm. With that large of an error it is doubtful that 5 significant figures could be claimed.

The real effect of adding significant figures is seen in comparing Tables 6-1 and 6-2 for the case of no error added (first line). In Table 6-1, which is the case of $\phi = 1^\circ$ and 4 significant figures, there is considerable error in ϕ , and particularly \bar{U} , even though there is no error in the input data. Increasing the accuracy of DM to 5 significant figures, as in Table 6-2, results in no error in the

screw axis parameters when no error is added to the "perfect data."

Table 6-6 shows that while ϕ could be determined with some accuracy, the determination of the components of \bar{U} was not possible for a rotation angle of 1° . This is consistent with the findings of Chapter 5. The problem is that the sine of a small angle is a small number, and dividing by that small number will magnify an error.

As would be expected, Table 6-6 reveals that as the rotation angle ϕ increases so does the accuracy of the screw axis parameters. Interestingly enough, errors in the translation, s , do not change as the rotation angle increases. In Table 6-6 it is seen that s is determined to within $\pm .10$ cm.

Examining Tables 6-1 through 6-5 reveals that the worst errors occurred when point 2 was perturbed. This is not surprising since point 2 is the closest of the three position data points to the origin of the created axis system. Recall that Chapter 4 indicated that the further a data point is from the origin of the axis system created based on the data points, the less effect an error in the data point has on the created axis system. The first data point is 38.9 cm from the origin, the second data point is 0.72 cm from the origin, and the third is 8.47 cm. Since point 2 is so close to the origin, an error in one of its coordinates will have a much greater effect on the coordinate system, thus on DM and the resulting screw axis

parameters.

The piercing point selected for this test was an arbitrary point. The screw axis direction was selected so that there would be equal components in all three dimensions. If a different screw axis orientation or location was selected the error effects might be different. This chapter is mainly to illustrate the effects of error, and give some idea of their magnitude. It should not be used as an indication of the maximum errors for a particular value of ϕ .

6.4 Evaluating Cond (P1)

The first point of interest is that $\text{cond}(P1)$ changes very little as error is added. It also does not change as the rotation angle is increased, for increasing the rotation angle does not effect the initial position, only the second position. Adding significant figures to the data does not change $\text{cond}(P1)$. It would seem on this basis that $\text{cond}(P1)$ is a function of the geometry of the targets. Using Table 6-1 and equation (5.9) it is now possible to evaluate the effects of an error in P1 on the error in DM. Since there are four significant figures (2 beyond the decimal point) assume

$$ep_1 = ep_2 = .005 \text{ per element}$$

From equation (5.10)

$$||e_{p1}|| = ||e_{p2}|| = .005 \sqrt{12} = .0173$$

From equation (5.9)

$$||e_{DM}|| = ||DM|| \text{ cond}(P1) \left[\frac{.0173}{76.81} + \frac{.0173}{77.04} \right]$$

$$= ||DM|| 4080 \times .00045 = 1.835$$

In this particular example $||DM|| = 2$

so


$$||e_{DM}|| = (1.835) (2) = 3.67$$

If it is assumed that e_{DM} is evenly distributed over all 16 elements of DM then the error in DM per element is

$$\frac{3.67}{\sqrt{16}} = .9175 \text{ or a } 91.75\% \text{ error} \quad (6.1)$$

Obviously, DM is known better than .9175. The assumption that the error is evenly distributed among all of the elements of DM may be unrealistic. It should also be kept in mind that Forsythe and Moler [11], who developed the equations which equation (5.9) is based on, were not trying

to define the error propagation, only to put an upper bound on the resulting error in a solution to a set of equations. In view of the answer in equation (6.1), does equation (5.9) have any real use in this error analysis? This question will be addressed in the final chapter.



CHAPTER 7

EXAMPLE OF SCREW AXIS ANALYSIS USING ANATOMICAL DATA

7.1 Introduction

This Chapter presents the results of a screw axis analysis performed using data collected from a cadaver in SAL. The joints analyzed are the hip, and the sacro-iliac joint. The bone movements analyzed are the femur moving relative to the left innominate for hip motion, and the sacrum moving relative to the innominate for the sacro-iliac joint.

The cadaver used was a Caucasian male who was 80 years old. The primary cause of death was a brain tumor and diagnostic radiographs revealed no abnormalities in the lumbar/pelvis/femur linkage system. During the studied motions the cadaver was supported by an overhead assembly which held the subject upright in a standing position.

Table 7-1 summarizes the screw axis analysis for the hip, and Table 7-2 summarizes the analysis for the sacro-iliac joint. In all cases the motion was from the same initial position of a supported erect posture with both feet on the floor. The motions analyzed were abduction, abducto-flexion (approximately equal amounts of abduction and flexion), and flexion. The final position was the extreme position of the indicated movement.

The motions studied were to the extreme positions. Since no intermediate positions were analyzed it is not possible to see the motion of the piercing point and/or screw axis. When joint mobility is studied, motions must be broken up into a number of small displacements. In this manner the motion of the screw axis may be studied.

7.2 Discussion

A summary of the screw axis analysis for hip motion is presented in Table 7-1. Note the large amount of translation which occurs. As much as 1.4 cm is seen in flexion. The analysis of Chapter 6 would indicate that these values are accurate to within $\pm .10$ cm. Since these motions were to the extreme positions, the movements of the femur were large, and the accuracy should be good. The classic model of the hip is a ball and socket joint. If the hip is a true ball and socket no translation should be observed. Note also that the range of values of $\text{cond}(P1)$ is 7800 to 2800.

This Chapter reveals that anatomical motions, such as those of the sacro-iliac joint, occur in the range where screw axis analysis is most sensitive to error. Table 7-2 presents the screw axis analysis for displacements between the extreme positions, yet the rotation angle is between 1° and 2° , and the translation is less than $\pm .15$ cm. Chapters 5 and 6 showed that the requirements for accuracy and the retention of significant digits, are most stringent for motions of the magnitude in Table 7-2.

TABLE 7-1 Screw Axis Analysis for Hip Motion

<u>Motion</u>	<u>s (cm)</u>	<u>φ (deg)</u>	<u>u_x</u>	<u>u_y</u>	<u>u_z</u>	<u>cond(P1)</u>	<u> P1 </u>	<u> P2 </u>
Abduction	-.07	24.0	.949	-.265	.171	7838	106.1	132.2
Abducto- flexion	-.46	44.5	.742	-.407	.532	3146	77.3	109.3
Flexion	1.44	55.6	.951	-.309	0.0	2783	72.21	128.39

TABLE 7-2 Screw Axis Analysis for the Sacro-iliac Joint

<u>Motion</u>	<u>s (cm)</u>	<u>φ (deg)</u>	<u>u_x</u>	<u>u_y</u>	<u>u_z</u>	<u>cond(P1)</u>	<u> P1 </u>	<u> P2 </u>
Abduction	.03	1.23	-.148	-.346	.926	4536	86.45	86.35
Abducto- flexion	.13	1.20	.339	.917	-.22	3821	84.71	84.57
Flexion	0.0	2.33	.985	.080	-.147	3431	80.75	80.43

Though these motions are small, they are important. Common engineering practice when modelling the human body, as with an anthropometric dummy, is to treat the pelvis as a rigid body and assume there is no motion in the sacro-iliac joint. The anatomical screw axis analysis presented in this Chapter indicates that motion occurred in the pelvis at the sacro-iliac joint.

CHAPTER 8
SUMMARY, REVIEW, AND RECOMMENDATIONS

8.1 Summary and Review

Present models of the human body generally make some simplifying assumptions to reduce the DOF present in a joint. However, human joints have a full six DOF, and any assumption which reduces these DOF artificially constrains the joint model or analysis.

The Displacement Matrix fully describes a three-dimensional displacement. DM maps a rigid body from one position to another. Screw axis analysis is a technique of making DM more easily understood. By specifying a vector \bar{U} which is the screw axis, a translation, s , parallel to the screw axis, and a rotation, ϕ , around the screw axis, any three-dimensional six DOF displacement can be described.

Chapter 4 discussed the data used to compute DM. In SAL the data consist of position coordinates of three points on a bone at two different positions P1 and P2. A coordinate system is set up based on the data points, and four new points on this coordinate system are used to compute DM. A coordinate system approach is used in order to insure an orthogonal RM. The coordinate system approach is effected by error, leading to the coordinate axes being

in the wrong location, or having the wrong orientation. The errors in the coordinate system are minimized by locating the data points used as equidistant from each other as possible, and by making the angle formed at the intersection of the relative position vectors as large as possible.

Given that there will be some error in the coordinate system, how does this error affect DM? And how does an error in DM effect the screw axis parameters? These questions were dealt with in Chapter 5. The problem of error propogation through matrix operations was discussed first. This is a complicated question, and a detailed analysis is outside the scope of this thesis. However, Chapter 5 developed a method for bounding the error propogation based on the condition number of a matrix.

An error in DM effects the screw axis analysis most when the rotation angle is small. While the determination of the rotation angle is sensitive to errors in DM, it is the determination of the components of \bar{U} , the unit vector in the direction of the screw axis, which is most sensitive to error.

Chapter 6 illustrates the theoretical error analysis of Chapter 5. By creating and then perturbing "perfect" position measurements it was possible to see how the screw axis parameters were effected. As expected the error for small rotation angles was large, and the error for large rotation angles was small. In general, rotation angles were determined with greater accuracy than Chapter 5 had

indicated, but the determination of \bar{U} was not possible at small angles. For small rotation angles, on the order of 1° , a minimum of four significant figures are needed to find ϕ to within an uncertainty of $\pm 0.41^\circ$.

In Chapter 6 an example indicating how the condition number could be related to expected errors in DM resulted in an exceedingly high error bound. The use of condition numbers is discussed in the next section.

This thesis describes a method of analyzing anatomical joint motion, and evaluates the limits of this method. As an illustration of what these anatomical studies might produce for screw axis parameters, Chapter 7 contains some analysis of joint mobility for a cadaver studied in SAL. The need for being able to accurately model small rotations was illustrated by the small rotations which occur in the sacro-iliac joint.

8.2 Is the Condition Number of a Matrix of Any Use?

From Chapter 6 it appeared that equation (5.9) produces an error bound which is too high to be useful. DM is known better than the $\pm 92\%$ computed using equation (5.9). Does this indicate the method is of no use? The interplay between measurement error and condition numbers is an area worthy of further study. This section presents some ideas which might serve as an introduction to such study, but for now equation (5.9) is not useful.

This thesis has used Euclidean norms in computing the condition number. This is in line with what Forsythe and

Moler [11] use, however, other norms can be used and are discussed by Forsythe and Moler. They also discuss methods of reducing the condition number, though they unfortunately conclude, "...it is quite unclear to us how to program a reasonable scaling of a general matrix." Scaling is a method of reducing the condition number. Two methods of scaling are discussed in Forsythe and Moler, the first involving pre-and post- multiplying by two different scaling matrices. The second method attempts to equilibrate the matrix in question.

The point of both scaling and equilibrating is to make the norms of the columns and rows of a matrix as close in value as possible. The closer the norms, the smaller the condition number, and the more accurately a solution is determined. The norms of the rows of one of the position matrices from Chapter 6 are given below.

Row 1 norm = 15.82

Row 2 norm = 3.45

Row 3 norm = 75.23

Row 4 norm = 2.0

Because the norm of the third row is so much larger than the other rows the condition number is large. The third row is composed of the z coordinates of the four points used to compute DM (refer to equation 3.4). The coordinates of the points are related to the location of the

origin of the coordinate system set up based on the anatomical data. While the x and y coordinates, in the inertial axis system, of the four points are close to the origin of the inertial system, the z coordinate is much further away. By relocating the origin of the anatomical axis system so that the z coordinate is closer in value to the x and y coordinate values, the condition number is reduced. This indicates that the condition number is a function of the geometry of the data used (the anatomical axis system) to solve for DM.

8.3 Recommendations for Future Work

Screw axis analysis is sensitive to errors at small rotation angles. It would seem then that whenever possible large rotation angles should be used. This is not a practical restriction for two reasons. First of all, as was seen in Chapter 7 much of the desired data are at small rotation angles.

The second reason might be termed the paradox of screw axis analysis. While small rotations and translations are prone to error, large rotations and translations yield a less than accurate description of the motion. If an air traveler catches a plane in New York, and is later seen in Los Angeles, the motion description would be from New York to Los Angeles. But what if the traveler went to Florida first, then London, then Chicago, and finally Los Angeles. His motion would be much different in this second case, but

if all that was available was a beginning and ending point, the path in between is not well known. It seems that the only way to use screw axis analysis is to acquire accurate data for small motions and retain five significant figures.

In Chapter 5 it was observed that even with no error in the data, when only four significant figures are available, a rotation angle of 1° can only be found to within $\pm 0.4^\circ$. Chapter 6 showed that for this same case the components of \bar{U} were adversely affected when only four significant figures were available, even when there was no error in the data. Increasing to five significant figures removed the error in the determination of the screw axis parameters. Chapter 7 pointed out that rotation angles on the order of 1° are to be expected in anatomical studies.

The algorithm for creating an axis system based on anatomical data does so without regard for the most accurate resulting coordinate system. It would be useful to create an algorithm which would compromise between placing the three data points as far from each other as possible, and making the included angle between the relative position vectors as close to 90° as possible. An appropriately selected coordinate system might reduce the effect of measurement error present in the position data.

There has been considerable discussion in this thesis of evaluating the error propagation through matrix operations. The ideas presented are only a beginning. The relationship between the condition number and the coordinate

system may lead to a method of reducing the error propagation through the matrix operations used to find DM. An optimization study where the function to be minimized is the condition number, might provide the optimum anatomical coordinate system for reducing error propagation. The independent variables would be the coordinates of the origin of the anatomical axis system, and two scaling matrices.

Another mathematical technique for reducing error propagation involves the use of surfaces. There should be much interest in screw axis surfaces. By passing a surface through all of the screw axes produced by a series of displacements the beginning of a joint model is created. Two surfaces are needed, one for the fixed object (the innominate in the analysis of Chapter 7) moving relative to the moving object (the femur in the analysis of Chapter 7). The second surface results from the motion of the moving object relative to the fixed object. The two surfaces produced would appear to roll in the direction normal to the axis common to the two surfaces, and to slide along the common axis [13,27]. If the geometry and location of the two surfaces is known, along with a definition of the amount of sliding, the spatial motion is uniquely defined [13,27].

The second and initially more useful feature of screw axis surfaces is that a surface smoothes data. An outlier from a screw axis surface could be in error, though actual slippage in the joint may also appear as an outlier. It would be interesting to select a screw axis from a smoothed

screw axis surface, and then reconstruct DM.

In a similar manner it would be useful to construct a surface based on all of the anatomical position data for one target. This surface would then represent a surface in space that is the locus of motion of a target on a bone. The smoothing effect of the surface should be an aid in dealing with measurement error, and the possibility of selecting positions not measured exists. The shape of the surface would also be of interest. If the hip is a ball and socket joint, all points of the femur should move on a sphere around the hip. It would be interesting to locate the center of such a sphere. If, as is more likely, the hip is not a perfect ball and socket, the shape of the surface would contain interesting and useful information.

If three points are the minimum needed to specify rigid body position could not many points be used? The points would be put into a position matrix and an overdetermined set of equations would result, allowing the use of a least squares analysis. Lennox and Cuzzi {16} report that this method does not improve the accuracy of screw axis analysis, but this question is still worth examining because of possible different measurement techniques used in SAL. Lennox and Cuzzi do report on a method of improving position data for use in screw axis analysis. Their method relies on photographic centers and might be worthwhile exploring for use in SAL. The author feels that an improved coordinate system algorithm would incorporate

some of Lennox and Cuzzi's ideas.

8.4 Conclusions

- 1) In order to contain measurement error to position data an anatomical axis system approach for computing DM should be used.
- 2) The origin of an anatomical axis system should be equidistant from all of the data points used to compute the anatomical axis system.
- 3) The bound on the error propagation due to the matrix operations used to find DM as developed in equation (5.9) is too high to be useful. Study of the propagation of measurement errors through matrix operations is an area worthy of future investigation.
- 4) If small rotation angles are to be analyzed, five significant figures are needed in the data.
- 5) As the rotation angle decreases the error propagation increases. This is not a linear function. If rotation angles on the order of 1° are to be studied, the elements of DM must be accurate to within $\pm .0002$ for an error in ψ of less than $\pm 0.5^\circ$.

- 6) Screw axis analysis requires accurate data. Either sophisticated measurement techniques must be used, or mathematical techniques must be developed to reduce the uncertainty in DM to less than ± 0.0002 .

- 7) Of the two methods suggested in Conclusion 6, it is recommended that mathematical techniques be used in the near future. Specifically, improved selection of an anatomical axis system for use in computing DM, and the use of surfaces are the most fruitful areas to explore.

LIST OF REFERENCES

LIST OF REFERENCES

1. Abbot, E. A., Flatland, Dover Press; 1963.
2. Baird, D. C., Experimentation: An Introduction to Measurement and Experiment Design, Prentice Hall, 1962.
3. Braune, W. and O. Fisher, "Die Bewegungen des Kniegelenkes nach einer neuen Methode am lebenden Menschen gemessen" (The Movements of the Knee Joint as Measured by a New Method in Living Humans), Abhandlungen der Mathematisch-Physischen Classe der Königl. Sachsischen Gesellschaft der Wissenschaften, 17: 75-150, 1891.
4. _____, "Bestimmung der Trägheitsmomente des menschlichen Körpers und seiner Glieder," Abh. d. Math. Phys. Cl. d. K. Sachs. Gesell., d. Wiss., 18(8): 409-492, 1892.
5. _____, "The Center of Gravity of the Human Body as Related to the German Infantryman," Leipzig, 1889, available from National Technical Information Service, AT1 138 452.
6. Bullock, M. I. and I. A. Harley, "The Measurement of three-dimensional body movements by use of photogrammetry," Ergonomics, 15(3): 309-322.
7. Chasles, M., "Note sur les propriétés générales du système de deux corps," Bulletin Sci. Math., Ferrusac 14:321-326, 1830.
8. Dempster, W. T., "The Anthropometry of Body Motion," Annals of the New York Academy of Science, 63:559-585, 1955.
9. _____, "Space Requirements of the Seated Operator," Wright Air Development Center, Technical Report 55-159, Wright Air Force Base, Ohio, 1955.

10. Emanuel S., and J. T. Barter, "Linear Distance Changes Over Body Joints," Wright Air Development Center, Technical Report 56-364, ASTIA Document #AD 1118003, 1957.
11. Forsythe, G. and C. B. Moler, Computation of Linear Algebraic Systems, Prentice Hall, 1967.
12. Hallert, B., "The Basic Geometric Principles of X-ray Photogrammetry," Transactions of the Royal Institute of Technology, 123:1-53, 1958.
13. Kinzel, G. L., On the Design of Instrumented Linkages for the Measurement of Relative Motion Between Two Rigid Bodies, Ph.D. Thesis, Purdue University, 1973.
14. Kinzel, G. L., A. S. Hall, Jr., and B. M. Hillberry, "Measurement of the Total Motion Between Two Body Segments, Part I - Analytical Development," The Journal of Biomechanics, 5:93-105, 1972.
15. _____, "Measurement of the Total Motion Between Two Body Segments, Part II - Description of Application," The Journal of Biomechanics, 5:283-293, 1972.
16. Lennox, J. B. and J. R. Cuzzi, "Accurately Characterizing a Measured Change in Configuration," ASME Paper No. 78-DET-50, 1978.
17. MacNeil, G. T., "X-ray Stereo Photogrammetry," Photogrammetric Engineering, 32:993-1004.
18. Potthoff, R. E., An Analysis of the Biomechanics of the Human Knee, M. S. Thesis, Stanford University, 1968.
19. Reuleaux, D. F., The Kinematics of Machinery, translated and edited by A. B. W. Kennedy, Dover Publications, 1963.
20. Reynolds, H. M., "A Foundation for Systems Anthropometry," Interim Report to United States Air Force Office of Scientific Research, AFOSR - TR - 77 - 0911, 1977.
21. Reynolds, H. M., J. Freeman, and M. Bender, "A Foundation for Systems Anthropometry, Phase II," Final Report to the Air Force, AFOSR - TR - 78 - 1160, 1978.

22. Reynolds, H. M., R. P. Hubbard, J. R. Freeman, and J. Marcus, "A Foundation for Systems Anthropometry, Phase III," interim report to the Air Force, 1979.
23. Reynolds, H. M., R. C. Hallgreen, and J. Marcus, "A Stereo Radiographic Measurement System for Systems Anthropometry," paper submitted to Journal of Biomechanics.
24. Robbins, D. H., "Errors in Definition of an Anatomically Based Coordinate System Using Anthropometric Data," p. 29-34 in Reynolds, H. M. "A Foundation for Systems Anthropometry, Phase I," reference 20 above.
25. Rogers, D. F. and J. A. Adams, Mathematical Elements for Computer Graphics, McGraw Hill, 1976.
26. Selvik, G., A Roentgen Stereophotogrammetric Method for the Study of the Kinematics of the Skeletal System, Ph.D. Thesis, University of Lund, Sweden, 1974.
27. Suh, C. H. and Radcliffe, C. W., Kinematics & Mechanism Design, John Wiley & Sons, 1978.
28. Thompson, C. T., A System for Determining the Spatial Motions of Arbitrary Mechanisms - Demonstrated on the Human Knee, Ph.D. Thesis, Stanford University, 1972.